THE ASTROPHYSICAL JOURNAL, 235: 76–84, 1980 January 1

OUTER ATMOSPHERES OF COOL STARS. III. *IUE* SPECTRA AND TRANSITION REGION MODELS FOR ALPHA CENTAURI A AND B

THOMAS R. AYRES[1] AND JEFFREY L. LINSKY[1,2]
Joint Institute for Laboratory Astrophysics, University of Colorado and National Bureau of Standards, Boulder, Colorado
Received 1979 April 9; accepted 1979 July 12

ABSTRACT

We describe *IUE* ultraviolet spectra of two nearby dwarf stars, α Centauri A (G2 V) and B (K1 V). These data include high-resolution profiles of the Mg II *h* and *k* features and lower-resolution integrated fluxes of lines from the following species: H I, C I–IV, N V, O I, Al II, Si II–IV, and Fe II. We find that surface fluxes in chromospheric and transition-region lines of α Cen A and B are nearly identical to those of the quiet Sun. In addition, the measured stellar line fluxes are in good agreement with predictions of a transition-region scaling law based on conductive heating and pressures estimated from chromospheric models of α Cen A and B. While this agreement does not verify the conductive heating hypothesis, it does suggest that the basic physical processes that control the structure and energy balance in the chromospheres and transition regions of α Cen A and B and the Sun are, on a gross scale, very likely the same.

Subject headings: stars: atmospheres — stars: chromospheres — stars: individual — stars: late-type — ultraviolet: spectra

I. INTRODUCTION

The nearby α Centauri system (G2 V + K1 V) is an ideal prototype for exploring stellar analogs of the solar chromosphere, transition region, and corona. The two components of the binary are the closest and brightest stars of their spectral classes. The system has been well observed by ground-based spectroscopy, photometry, and astrometry (see Kamper and Wesselink 1978 and references therein). The system is comparable in age to the Sun and has a very similar galactic orbit (Flannery and Ayres 1978). Except for small structural differences caused by a 10% larger mass and CNO abundances possibly enhanced by a factor of 2, α Cen A is virtually identical to the Sun. On the other hand, α Cen B is considerably different. It is smaller, cooler, and less luminous than the Sun, but has a substantially deeper and more massive convection zone.

A previous study of α Cen A and B by Ayres *et al.* (1976), based on the Ca II λ3934 K resonance line, suggested that the low chromospheres of the two stars are very similar to each other and to that of the Sun. In addition, the α Centauri system has been detected recently in soft X-rays by *HEAO 1* (Nugent and Garmire 1978). The apparent coronal emission from the binary is comparable to that of the average Sun (Ayres *et al.* 1978; Topka *et al.* 1979), although the estimated plasma temperature is somewhat cooler than that of the solar corona.

In this paper, we present and analyze ultraviolet emission spectra of α Cen A and B. These data were obtained with the *International Ultraviolet Explorer* (*IUE*) (Boggess *et al.* 1978*a*). The initial in-flight performance of the *IUE* and the first observations of late-type stars are described by Boggess *et al.* (1978*b*) and by Linsky *et al.* (1978).

The *IUE* long-wavelength (2000–3200 Å) spectrograph covers the spectral range containing the 2800 Å Mg II *h* and *k* resonance lines, which are formed in the middle chromosphere. The *IUE* short-wavelength (1175–2000 Å) spectrograph covers the spectral range containing emission lines of H I, O I, and Si II, which are formed in the middle and upper chromosphere, as well as lines of C II–IV, Si III–IV, and N V, which are formed in hotter layers, presumably analogous to the solar transition region (TR) (see Noyes 1971). The *IUE* therefore fills the spectral gap between ground-based observations of the chromospheric Ca II H and K features and spacecraft measurements of coronal emission in soft X-rays.

In § II, we describe the *IUE* observations of α Centauri. In § III, we compare measured fluxes in prominent chromospheric and TR lines of α Cen A and B with the corresponding emission features from the solar spectrum and with previous predictions based on chromospheric models derived to match Ca II K line observations only. Finally, in § IV, we speculate on implications of these comparisons for understanding the chromosphere-corona phenomenon in the Sun and in other stars.

II. ULTRAVIOLET OBSERVATIONS

a) *Previous Work*

The Lα and Mg II *h* and *k* resonance lines of α Cen A have been observed previously with *Copernicus*

[1] Guest Observer, *International Ultraviolet Explorer*.

[2] Staff member, Quantum Physics Division, National Bureau of Standards.

(Dupree 1974, 1976; Dupree and Shipman 1976; Dupree, Baliunas, and Shipman 1977). Dupree and Shipman have shown that the α Cen A Lα feature is similar to that of the quiet Sun except that the stellar profile may be somewhat broader and the central portion of the emission core is obliterated by interstellar H I absorption. The Mg II resonance lines in α Cen A are also similar to the solar features. For example, the full width at k_1 ($W_1 = 2\Delta\lambda_{k_1}$ km s^{-1}) given by Dupree (1976, Fig. 4) is log $W_1 \approx 2.15$ for α Cen A, compared to the mean quiet-Sun value, log $W_1 = 2.19 \pm 0.05$, given by Ayres, Linsky, and Shine (1975). To our knowledge, α Cen B has not been observed previously in the ultraviolet.

The Ca II resonance lines have been measured at high dispersion in both components of α Centauri by Boesgaard and Hagen (1974) and by Ayres *et al.* (1976). The α Cen A K line profile is very similar to integrated sunlight profiles, except that the α Cen A emission core is about 10% wider. The K line of α Cen B shows a much larger K_2 peak-to-K_1 minimum contrast than does the solar (or α Cen A) feature, but the integrated core surface flux,

$$\mathscr{F}_K = \int_{\lambda_{K_{1v}}}^{\lambda_{K_{1r}}} \mathscr{F}_\lambda d\lambda \,, \tag{1}$$

is comparable. The greater contrast of the α Cen B K line emission core, compared with those of the Sun and α Cen A, results from the greater contrast in α Cen B between chromospheric temperatures, which control the strength of the emission core, and photospheric temperatures, which control the brightness of the inner wings and the K_1 minimum features. Chromospheric temperatures in α Cen B and the Sun are similar, whereas photospheric temperatures are systematically 500 K cooler in the K dwarf. The gross appearance of the α Cen B Ca II features does not imply that α Cen B has a more active chromosphere than α Cen A or the Sun. Instead, the total chromospheric radiative loss rates are very similar in these three stars (see Linsky and Ayres 1978).

b) *IUE Observations*

We obtained spectra of α Centauri on 1978 August 17. The observations are summarized in Table 1. The 21″ separation and similar brightness ($\Delta V \sim 1.3$ mag) of α Cen A and B presented some special problems for target acquisition and guiding. The normal acquisition sequence involves a coarse slew to the approximate coordinates of the star, and then final location of the target in the Fine Error Sensor (FES) field of view by directing the FES to find the center of light of the apparent stellar image. For α Centauri, the center of light of the FES image lies between the two components, and both stars would lie outside even the large aperture (10″ × 20″). Instead, we acquired α Cen A as a blind offset from the nearby star SAO 252855, and acquired α Cen B as a blind offset from α Cen A. During observations of one component, we used the other as a guide star.

Another difficulty in observing ultraviolet spectra of cool stars with the *IUE* is the limited dynamic range of the vidicon detectors (~30:1). This range is small compared with the large contrast between the brightest lines (Lα, O I, C II) and other important but weaker emission features shortward of 1600 Å. In addition, the stellar continuum rises rapidly longward of 1600 Å in solar-type stars and several important emission features are superposed on the steeply sloping background. In order to cover the expected intensity contrasts in α Cen A, we obtained three short-wavelength exposures of 30 minutes (image SWP 2315), 10 minutes (SWP 2317), and 1 minute (SWP 2318). Because the continuum region longward of 1600 Å is much weaker in the cooler K dwarf, two exposures, 4 minutes (SWP 2319) and 40 minutes (SWP 2320), were sufficient to cover the intensity range in α Cen B. All of the α Centauri short-wavelength spectra were recorded in the low-dispersion mode, since high-dispersion observations comparable with those obtained previously for Capella (Linsky *et al.* 1978) would have required excessively long exposures (~8 hr for α Cen A). (A 107 minute high-dispersion, short-wavelength exposure of α Cen A was obtained on 1978 August 16. As

TABLE 1

SUMMARY OF *IUE* OBSERVATIONS[a]

Star	*IUE* Image	Exposure Time (minutes)	Dispersion	Begin (UT)
α Cen A...........	LWR 2093	2	Hi	03:44
α Cen A...........	LWR 2094	1	Hi	05:03
α Cen A...........	SWP 2315	30	Lo	03:57
α Cen A...........	SWP 2317	10	Lo	07:20
α Cen A...........	SWP 2318	1	Lo	08:21
α Cen B...........	LWR 2095	6	Hi	08:58
α Cen B...........	LWR 2096	1.5	Hi	09:34
α Cen B...........	LWR 2097	18	Hi	10:03
α Cen B...........	SWP 2319	4	Lo	10:29
α Cen B...........	SWP 2320	40	Lo	11:00

[a] All observations were on 1978 August 17 using the large aperture.

expected, this spectrum is only weakly exposed shortward of 1600 Å, although the Lα profile is of good quality, and emission lines longward of 1800 Å are saturated.)

We also obtained high-dispersion spectra of the long-wavelength region (2000–3200 Å) in both stars as described in Table 1. The prominent chromospheric features in these data are the Mg II resonance doublet near 2800 Å, and the Mg I resonance line near 2850 Å. The Mg II h and k emission profiles described below are taken from a 1 minute exposure of α Cen A (image LWR 2094) and a 1.5 minute exposure of α Cen B (LWR 2096).

c) *Calibration of Spectra*

i) Mg II *h and k*

The long-wavelength spectra in the region containing the Mg II h and k lines were placed on an absolute flux scale by comparing the appropriate echelle orders with observations of the standard star η UMa. The calibration procedure is described in detail by Basri and Linsky (1979). The calibrated Mg II h and k lines of α Cen A and B are illustrated in Figure 1. Relative to the chromospheric emission cores, the photospheric wings of h and k are darker in α Cen B than in α Cen A. Nevertheless, the integrated core surface fluxes of the h and k features are virtually identical in α Cen A and B (see Table 3). The apparent behavior of the Mg II resonance lines is analogous to that of Ca II H and K described in § II*a*.

We have also measured characteristic widths of the stellar Mg II profiles. These are listed in Table 2 and compared with corresponding mean solar values (disk center and limb) obtained from the rocket spectra of

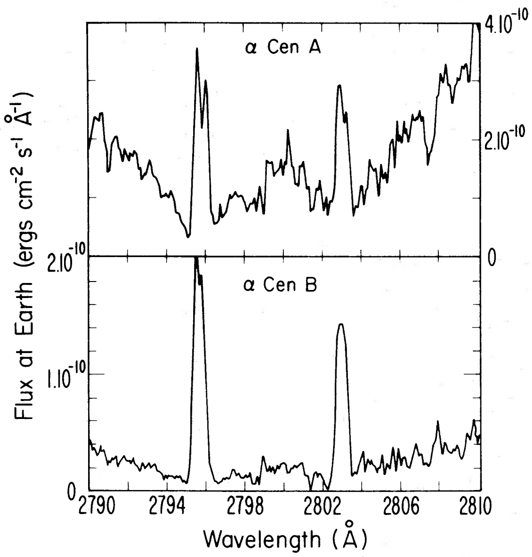

FIG. 1.—Profiles of the Mg II λ2803 h and λ2796 k resonance doublet in α Cen A and B. Note that the flux ordinate for α Cen A is twice that for α Cen B: This is equivalent to a comparison of *surface* flux profiles since the angular area of α Cen A is about twice that of α Cen B.

TABLE 2

Mg II LINE FULL WIDTHS (Å)

Feature	W (α Cen A)	W (α Cen B)	W[a] (Sun)
h_1	1.0	1.1	0.9–1.0
k_1	1.2	1.4	1.2–1.3
h_2	uncertain	uncertain	0.3–0.4
k_2	0.4	0.25	0.3–0.4
FWHM(h)	0.7	0.6	0.5–0.6
FWHM(k)	0.8	0.7	0.5–0.7

[a] Kohl and Parkinson 1976, Tables 2 and 3. First entry is for the quiet Sun at disk center, and the second entry is for the quiet Sun near the limb (μ = 0.23).

Kohl and Parkinson (1976). The α Cen A k_1 separation obtained here (1.2 Å) is somewhat smaller than the 1.3 Å value obtained by Dupree (1976) from *Copernicus* spectra, but this difference is within expected errors of measuring Mg II base emission widths. If we allow for the lower resolution of the *IUE* spectra (0.2 Å versus 0.02 Å), the α Cen A widths for h and k are very similar to those of the corresponding solar intensity profiles. (Note that a solar-flux profile would have characteristic widths lying between those of disk center and limb intensity profiles.)

ii) *Short-Wavelength Region*

Calibrations and scattered-light corrections.—The short-wavelength spectra of α Cen A appear to contain some scattered light, probably originating in the bright continuum longward of 1900 Å. To make a crude correction for the scattered-light background, we assumed it to be independent of wavelength and equal to the emission level shortward of 1150 Å. Any flux in that region must be spurious because the intrinsic continuum emission from a solar-like dwarf is extremely faint shortward of 1200 Å and because the MgF_2–coated optics have very poor reflectance shortward of about 1150 Å. Scattered light is much less of a problem in the α Cen B spectra because the implicated source of the stray light—the continuum longward of 1900 Å—is much weaker in the K dwarf compared with α Cen A or the Sun. The extent to which the scattered-light background departs from the assumed wavelength-independent behavior is unknown and cannot readily be determined from our data alone.

Next, the individual short-wavelength exposures of α Cen A (or B) were shifted to fit a common wavelength scale derived from positions of the prominent emission features O I λ1305, C II λ1335, and C IV λ1550. The registered spectra were then co-added to form a single cumulative exposure. Regions of the individual spectra that were saturated or affected by reseau marks were omitted from the superposition, and the cumulative exposure times for these intervals were reduced accordingly. For example, the cumulative exposure in the bright continuum region longward of 1700 Å in α Cen A is just that of the shortest exposure, since the two longer exposures of that region are both at least partially saturated. Conversely, the cumulative exposure in the immediate vicinity of the N V λ1240 resonance doublet is the sum of the three individual exposure times, since all of the vidicon images of this intrinsically faint region are unsaturated. Finally, we multiplied the superposed spectra by the inverse sensitivity curve S_λ^{-1} for the short-wavelength prime spectrograph (Bohlin *et al.* 1979) and divided by the cumulative exposure time. The resulting spectrum is calibrated in absolute flux units at the Earth. These data are compared in Figure 2 with the integrated disk quiet-Sun spectrum (Rottman 1978) as it would appear at a distance of 1 pc, degraded to the approximate 6 Å FWHM resolution of the *IUE* short-wavelength spectrograph.

The overall similarity between the ultraviolet spectra of the Sun and α Cen A is striking. The prominent emission features have about the same relative strength in both spectra, and there are no prominent lines in α Cen A that appear to be anomalously strong or weak compared with the Sun. Also, the photospheric continuum emission longward of 1700 Å is virtually identical in α Cen A and the Sun. The close similarity between ultraviolet continuum emission in the two stars supports the conclusion of Flannery and Ayres (1978), based on broad-band infrared color indices, and the suggestion of Doherty (1972), based on *OAO 2* data, that α Cen A and the Sun have nearly identical effective temperatures.

The ultraviolet emission-line spectrum of α Cen B is also qualitatively similar to that of the Sun and α Cen A. In fact, the comparison is *quantitative* because the *apparent* fluxes of the α Cen B emission lines at the Earth should be about half those of α Cen A if both stars have comparable surface fluxes, since α Cen B has only about half the surface area of α Cen A. The most obvious difference between the spectra of α Cen A and α Cen B is the continuum region longward of 1700 Å. The surface flux from α Cen B near 1950 Å is more than an order of magnitude smaller than that of α Cen A or the Sun. As a result of the reduced photospheric background emission in α Cen B, the Si II triplet feature at 1815 Å is more prominent in the K dwarf spectrum than in the hotter spectra of the Sun and α Cen A. Note that the large drop in continuum emission near 1900 Å in α Cen B relative to α Cen A is the result of a difference in effective temperatures of only 500 K.

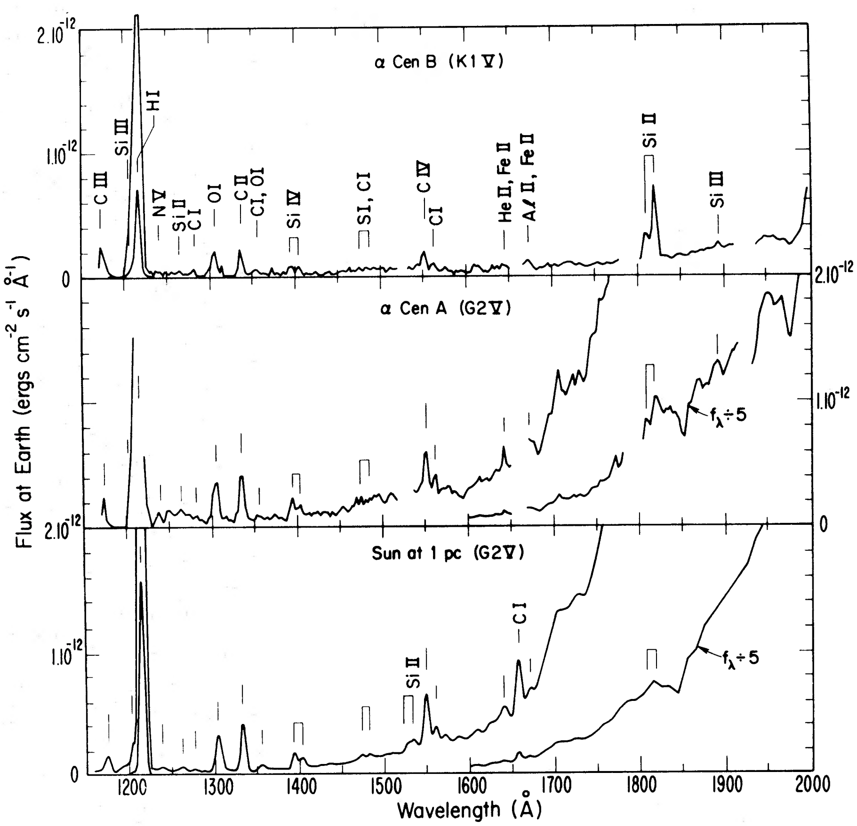

FIG. 2.—Comparisons of *IUE* short-wavelength spectra of α Cen A and B with a spectrum of the integrated solar disk as it would appear at a distance of 1 pc. Note that the Sun at 1 pc has essentially the same angular area as α Cen A; hence the comparison of *apparent* fluxes is also a comparison of *surface* fluxes. Positions of prominent spectral features are indicated. The Lα features of α Cen B and the Sun are shown at full scale and divided by 10. The photospheric continuum regions longward of 1600 Å in α Cen A and the Sun are shown at full scale and divided by 5. Gaps in the α Centauri spectra are regions affected by saturation (e.g., Lα in α Cen A) or by reseau marks.

Short-wavelength line identifications.—In Table 3 we summarize tentative identifications of prominent spectral features in the short-wavelength regions of α Cen A and B. We have relied primarily on line lists for the quiet-Sun spectrum off-limb (Burton and Ridgeley 1970), for a coronal hole off-limb (Feldman *et al.* 1976), for active regions off-limb (Feldman and Doschek 1978*a*), and for solar flares (Cohen, Feldman, and Doschek 1978). Since the spectral resolution in the low-dispersion mode is only 6 Å FWHM, we have paid special attention to the problem of blending. We first identified prominent features in a 1 Å resolution rocket spectrum of the integrated solar disk (Rottman 1978), and then deduced which lines are the primary contributors to blends in the same spectrum degraded to the *IUE* resolution (see Fig. 2). For example, the weak feature near 1350 Å is a blend of several moderately strong transitions of neutral carbon and oxygen. The most prominent features in all three spectra are the resonance lines of H I λ1216, O I λλ1302, 1305, 1306, C II λλ1334, 1335, Si IV λλ1394, 1403, C IV λλ1548, 1551, and Si II λλ1808, 1816, 1817. The C III λ1175 profiles in α Cen A and B also appear to be prominent, but the strength of these features may be at least partially spurious; since the inverse sensitivity curve for the short-wavelength prime cameras rises rapidly toward shorter wavelengths below 1200 Å, small noisy features in the raw spectrum can be amplified in the calibrated spectrum. Furthermore, the C III feature in α Cen A is narrower than might be expected on the basis of the appearance of the blended multiplet in the degraded solar spectrum, and the C III features in both α Cen A and B peak slightly shortward of the expected wavelengths. The N V resonance doublet near 1240 Å appears to be present in both α Cen A and α Cen B, although the features are weak and occur in a region where there is extensive, faint spectral structure. The N V doublet, formed near $T \sim 2 \times 10^5$ K, is important because it is the "hottest" feature that is readily accessible in the short-wavelength *IUE* spectra.

We note that there are weak features in both the α Cen A and B spectra near 1370 Å that have no obvious counterpart in the degraded solar spectrum. These features could be O V λ1371, which is formed at about the same temperature as the N V λ1240 doublet. If so, the O V line surface fluxes in both stars are roughly 6 times the quiet-Sun flux. However, if there is substantially more material near $T \sim 2 \times 10^5$ K in α Centauri compared with the Sun, we would expect the N V features to be correspondingly enhanced. Such an enhancement is not apparent in Figure 2. We would

TABLE 3

LINE SURFACE FLUXES

Wavelength (Å)	Identification	Line Surface Fluxes (ergs cm^{-2} s^{-1}) α Cen A	α Cen B	Sun	α Cen/Sun
1175	C III?	2.6 (3):	1.0 (4):	1.6 (3)	1.6:
1216	H I Lα + Si III 1206	SAT	3.0 (5)[a]	[2.3 (5)][c]	1.3
1240	N V	1.6 (3):	2.0 (3):	8.5 (2)	2.1:
1264	Si II	2.8 (3):	2.1 (3):	1.1 (3)	2.2:
1275	C I	1.2 (3):	2.4 (3):	5.2 (2)	2–5:
1304	O I	7.2 (3)	9.1 (3)	4.0 (3)	2.0
1310	Si III?	...	1.6 (3):	...	...
1335	C II	7.2 (3)	7.0 (3)	4.6 (3)	1.5
1355	C I + O I	1.1 (3)	2.8 (3):	3.4 (2)	3–8:
1371	O V?	9.3 (2):[b]	9.7 (2):	[1.6 (2)][d]	6:
1394	Si IV	5.1 (3)[b]	5.4 (3)	2.5 (3)[b]	2.1
1403	Si IV + O IV				
1550	C IV	7.2 (3)[b]	7.5 (3)[b]	5.8 (3)[b]	1.3
1561	C I	3.0 (3):[b]	4.0 (3)[b]	2.0 (3)[b]	1.8
1640	He II + Fe II	2.1 (3):[b]	...	1.3 (3)[b]	1.6:
1657	C I	... reseau mark ...		5.3 (3)[b]	...
1670	Al II + Fe II	...	4.7 (3):[b]	1.5 (3)[b]	3.1:
1705, 10	Fe II?	4.9 (3)[b]	...	...	...
1721, 29	Fe II?	3.0 (3)[b]	...	...	...
1808	Si II	2.1 (4)[b]	3.1 (4)[b]	[1.6 (4)][b,e]	1.6
1817	Si II				
1892	Si III + Fe II	1.9 (4):[b]	2.2 (3)[b]	...	...
2796	Mg II k	6.1 (5)	7.5 (5)	[6.0 (5)][f]	1.1
2803	Mg II h	5.4 (5)	5.1 (5)	[4.5 (5)][f]	1.2
3934	Ca II K	[4.4 (5)][g]	[4.2 (5)][g]	[4.2 (5)][f]	1.0

[a] No correction for interstellar Lα absorption or geocoronal emission.

[b] Background continuum subtracted.

[c] For mean solar Lα irradiance of 5 ergs cm^{-2} s^{-1} at Earth (e.g., Vidal-Madjar 1977, Table 4).

[d] $\mathscr{F}_l \approx \pi I_l$; I_l from Kjeldseth Moe and Nicolas 1977.

[e] Linsky *et al.* 1978.

[f] Linsky and Ayres 1978; Ayres and Linsky 1976.

[g] Ayres *et al.* 1976.

also expect strong O VI emission, but the 1032 Å resonance line of O VI has not been seen in *Copernicus* spectra of α Cen A (Dupree 1976) at flux levels comparable to the quiet Sun at 1 pc.

Finally, we point out the weakness of the He II–Fe II blend near 1640 Å in α Cen B relative to α Cen A and the Sun.

Surface fluxes.—In order to compare quantitatively the α Centauri and solar ultraviolet spectra, we have estimated surface fluxes for many of the prominent emission lines. We first integrated the apparent fluxes $f_\lambda^\oplus$ in a particular spectral feature, and then multiplied by the inverse geometrical dilution factor $(d_*/R_*)^2$ to convert from flux at the Earth to surface flux at the star. We assumed a distance of 1.33 pc derived from the measured parallax (Kamper and Wesselink 1978), and radii $R_A = 1.23\ R_\odot$ and $R_B = 0.80\ R_\odot$ based on the measured luminosities of the binary components and effective temperatures inferred from broad-band infrared color indices (Flannery and Ayres 1978).

Several spectral features, the Si IV and C IV doublets in α Cen A, for example, are superposed on a steeply sloping continuum originating in the stellar upper photosphere and low chromosphere. For these lines, an estimated linear background level was interpolated across the bottom of the line profile and subtracted. The same techniques applied to the α Centauri spectra were also applied to the degraded solar spectrum so as to minimize any systematic effects in our comparison of these stars with the Sun arising, for example, from blending or the continuum interpolation procedure.[3]

The derived emission-line surface fluxes for α Cen A, α Cen B, and the mean Sun are listed in Table 3. Many of these fluxes are uncertain owing to the weakness of the measured feature. Also, fainter lines are more affected by errors in the scattered-light correction and in the continuum interpolation procedure than are strong lines. Those fluxes in Table 3 that are uncertain are indicated by colons. (Unfortunately, we have no way at present of quantitatively assessing measurement errors for the weak lines, owing to the unknown frequency dependence of the scattered-light background, and the unknown amount of contamination of the interpolated continuum level by faint emission lines.)

III. DISCUSSION

a) *The Solar Transition Region—An Overview*

The solar transition region (TR) is a thin interface that separates the cool chromosphere ($T \sim 6 \times 10^3$ K) from the hot corona ($T \sim 2 \times 10^6$ K) (e.g., Noyes 1971). The transition region is characterized by steep temperature gradients and is narrower than a vertical pressure scale height at its base temperature, $T_0 \approx 2 \times 10^4$ K. As a result, the gas pressure $P_0 = 2nkT$ (where n is the electron density at temperature T) is essentially constant across the TR. The surface flux, $\mathscr{F}_l$, emitted by a collisionally excited optically thin resonance line formed in a plane-parallel homogeneous TR, is proportional to

$$\mathscr{F}_l \sim A_{\rm el} P_0^2 \langle (dT/dz)^{-1} \rangle\,, \tag{1}$$

where $A_{\rm el}$ is the element abundance relative to hydrogen and $\langle (dT/dz)^{-1} \rangle$ is an average of the inverse vertical temperature gradient across the region of line formation (e.g., Withbroe 1977). Since any given ionization stage typically has a significant concentration over only a small range of $\Delta T/T$, the thermal integrations over height implicit in equation (1) are relatively straightforward and can be evaluated without a detailed knowledge of the model temperature structure. Therefore, the integrated fluxes in a set of emission lines formed over a range of temperatures can tell us the distribution of temperature gradient with temperature if we have an estimate of the coronal base pressure P_0 by an independent method and if we know the relative abundances $A_{\rm el}$. Finally, an integration of $(dT/dz)^{-1}$ over temperature determines a plane-parallel empirical model $T(z)$ of the transition region, with a constant pressure given by the particular value of P_0. Given such a model we could hope to infer the underlying energy balance mechanisms that control the structure of the TR in the Sun or in a star such as α Cen A.

Alternatively, we could impose conditions on the energy balance in a TR model that would imply a relationship between the local temperature gradient, the base pressure, and the local temperature. We could then explicitly evaluate the inverse vertical temperature-gradient average in equation (1), and from measured line fluxes we could, for example, determine empirically a value of P_0. Until recently, the most common condition placed on solar TR models has been the assumption that the temperature structure is controlled by heat conduction from the overlying hot corona. This assumption was based on both empirical and theoretical arguments. Empirically, Pottasch (1964) and Athay (1966), among others, have shown that derived TR temperature distributions based on disk-average emission-line fluxes are consistent with conductive heating. One important theoretical argument is that the 2×10^6 K corona is far from the temperature of maximum radiative efficiency in a dilute plasma since the cooling rate decreases with increasing temperature between 10^5 and 10^7 K (see Cox and Tucker 1969). Consequently, the corona should be unstable if radiation were the only loss mechanism. Nevertheless, bright structures within the corona appear to be quite stable. The brightest and hottest structures of the solar corona are regions with closed magnetic field geometries, which severely

[3] As a result of the substantial decrease in the sensitivity of the rocket spectrometer (Rottman 1978) near 1700 Å, the solar fluxes longward of that wavelength are the 10 Å averages cited in Heath and Thekaekara (1977). These irradiance data are *not* suitable for comparisons with stellar emission lines, although they are valuable for comparing the continuum energy distributions. Therefore, solar line fluxes longward of 1700 Å were not determined directly from the degraded spectrum, but instead were taken from other sources, such as Linsky *et al.* (1978). This was also done for several lines shortward of 1700 Å, which appear to be present in the α Centauri spectra, but which are not obvious in the degraded solar spectrum, for example, O V λ1371.

inhibit energy loss via the solar wind (see Vaiana and Rosner 1978). The only remaining obvious heat-loss mechanism is electron conduction down along the magnetic field lines. Since the flux carried by conduction is proportional to both the temperature and the temperature gradient, $\mathscr{F}_c \sim 10^{-6}T^{5/2}dT/dz$ (Ulmschneider 1970), thermal conduction can balance nonradiative heating at the observed coronal temperatures while radiation alone cannot. In this picture, the TR temperature distribution is determined by the dissipation of the downward flux of coronal heat by radiative cooling, which is a much more effective loss mechanism in the cooler, denser layers of the upper chromosphere and TR than in the corona itself. Withbroe (1977) has shown that if radiative losses balance the divergence of the conductive flux in the TR and if the entire coronal heat flow to the TR is removed by radiation within the TR, then the local temperature gradient at each height should be proportional to the base pressure P_0 and to a simple function of temperature that depends on the details of the plasma radiative cooling curve.

b) The Transition Regions of α Centauri A and B

Assuming the heat-conduction–dominated plane-parallel TR model, we predicted that stellar resonance-line emission fluxes should scale from solar values roughly as $\mathscr{F}_l \sim A_{\rm el}P_0$ (Ayres *et al.* 1976). The pressure effect is demonstrated by the difference in emission-line intensities between the quiet Sun and active regions: line strengths are enhanced in active regions and flares by factors of 10–100 compared with the quiet Sun, and coronal base pressures, as inferred from density-sensitive line ratios, appear to be enhanced by similar factors (Vernazza and Reeves 1978; Feldman and Doschek 1978*b*).

We now consider whether the simple $\mathscr{F}_l \sim A_{\rm el}P_0$ scaling law is applicable to α Cen A and α Cen B. Table 4 compares line fluxes measured from the *IUE* spectra with the Ayres *et al.* (1976) predictions. In the earlier work, we estimated the coronal base pressures for both components of α Centauri from chromospheric models constructed to match the emission cores of calibrated Ca II line profiles. We assumed that the pressure at the "top" of the model chromosphere near 8000 K is the same as the coronal base pressure, since in analogy with the Sun we expected that both the upper chromosphere and TR would be relatively thin compared with a pressure scale height. The striking agreement between the predictions and observed line fluxes for the strong, and therefore most accurately measured, features in both α Cen A and B is a clear indication that the outer atmospheres of these stars are quantitatively similar to that of the Sun. Differences between the observed and predicted fluxes of the weaker lines are probably not significant, owing to the large measurement uncertainties for the weak features.

We also include in Table 4 comparisons of predicted Mg II resonance-line fluxes based on the Ayres *et al.* (1976) chromospheric models, with integrated *h* and *k* fluxes measured from the profiles illustrated in Figure 1. The agreement is excellent for α Cen B, but somewhat poorer for α Cen A.

We feel that the reasonable agreement between predictions and measured Mg II fluxes for the two stars demonstrates that the values of P_0, determined by computing chromospheric models to match the Ca II emission cores, are not grossly in error. In particular, the Mg II emission features are formed higher in the chromosphere than the analogous Ca II cores, and should be more sensitive indicators of the upper chromosphere "boundary" pressure than the Ca II lines.

Despite the striking agreement between the 1976 scaling-law predictions, based on the conduction-dominated TR model, and the observed fluxes of TR lines in α Centauri, the assumed TR model is very likely oversimplified. In fact, it is not clear that the solar TR is heated solely by thermal conduction, particularly at temperatures below about 10^5 K. Withbroe (1977) has pointed out that radiative losses in the layers below about 10^5 K are too large to be balanced only by the residual heat flux conducted down through the overlying atmosphere. Additional heating of the lower TR layers by a mechanical energy flux appears to be necessary. Furthermore, the greatly improved spatial resolution of the *Skylab* ATM

TABLE 4

PREDICTED AND OBSERVED LINE FLUXES AT EARTH (photons cm^{-2} s^{-1})

Transition	α Centauri A		α Centauri B	
	Predicted[a]	Observed[b]	Predicted[a]	Observed[b]
Si III 1206	0.12	...	0.059	...
N V 1240[c]	0.018	0.042:	0.0089	0.024:
Si II 1265[c]	0.025	0.076:	0.013	0.025:
C II 1335[c]	0.19	0.21	0.10	0.087
Si IV 1400[c]	0.10	0.16	0.050	0.070:
C IV 1550[c]	0.27	0.24	0.13	0.11
Mg II 2800[c]	44	69	30	34

[a] Ayres *et al.* 1976.

[b] This work.

[c] Includes both members of the doublet.

experiments revealed that much of the solar ultraviolet emission is concentrated in discrete structures, rather than distributed uniformly over the solar surface. In supergranulation network boundaries, for example, enhanced emission in discrete structures relative to surrounding areas is not accompanied by the equally enhanced TR pressures that are required by the conduction-dominated hypothesis. In addition, there are classes of transient phenomena, for example, cool plumes of plasma over sunspots (Foukal 1975), that have greatly enhanced radiation in 10^5 K lines without greatly enhanced pressures. We conclude that while the conduction-dominated TR model is successful in explaining many of the gross characteristics of spatially and temporally averaged solar EUV spectra, the actual physical configurations and energy balance of high-temperature regions in the solar atmosphere are vastly more complex. An understanding of the structure of these regions must include a realistic treatment of the magnetic fields that permeate the TR and coronal plasma, particularly the roles played by the field geometry in both inhibiting and channeling heat conduction and bulk plasma flows (Pneuman 1973; Gabriel 1976). In addition, a more detailed consideration of dynamical phenomena is needed, particularly heat transport by enthalpy flows (Pneuman and Kopp 1978).

The close agreement between the 1976 predictions and 1978 observations should not, therefore, be taken as a confirmation of the conduction-heated models, but rather as an indication of the similarity, if not universality, of the underlying physical mechanisms that create and maintain TRs in stars like the Sun.

In fact, this similarity may extend to stars much different from the Sun. Linsky and Haisch (1979) have presented evidence that TRs are a common phenomenon over a wide band in the HR diagram, including F–K dwarfs and G giants. Doschek *et al.* (1978) have proposed that the similarity in shape of differential emission measure curves ($5 \times 10^4 \leq T \leq 2 \times 10^5$ K) in the quiet and active Sun and in a range of stars suggests a common physical basis for the underlying TR energy balance.

The similarity between the outer atmospheres of the Sun and α Cen A and B provides an ideal opportunity to test a subtle aspect of the solar chromosphere-corona, namely, activity cycles. Since α Cen A is nearly a twin of the Sun in both size and age, we expect that α Cen A should have a dynamo-driven activity cycle (Parker 1955; Babcock 1961) similar to that of the Sun. Since α Cen B is somewhat different from α Cen A in terms of physical size and luminosity, and particularly with respect to the depth of its hydrogen convection zone, we might expect a somewhat different activity cycle for α Cen B. Long-term photometric studies of chromospheric activity indicators, such as the pioneering work by Wilson (1978) using the Ca II H and K lines, or soft X-ray monitoring (Topka *et al.* 1979), should tell whether the activity cycles in α Cen A and B are similar to or different from the well-studied solar cycle.

Finally, we have considered only the transition regions of the α Centauri stars. The apparent similarities between chromospheres and TRs in the Sun and the two components of α Centauri would seem to suggest that both stars have hot coronae (2×10^6 K) identical to that of the Sun. The α Centauri system has been detected as a soft X-ray source by *HEAO 1* (Nugent and Garmire 1978), indicating that one or both stars have a bright corona. However, the plasma emission temperature inferred from the shape of the pulse height spectrum is only about 5×10^5 K, which is considerably cooler than the solar corona, and may imply the existence of substantially different coronal structures.

We thank Dr. K. Gebbie for her comments on our paper, and we gratefully acknowledge support of NASA under grants NAS 5-23274 and NGL 06-003-057 to the University of Colorado.

REFERENCES

Athay, R. G. 1966, *Ap. J.*, **145**, 784.
Ayres, T. R., and Linsky, J. L. 1976, *Ap. J.*, **205**, 874.
Ayres, T. R., Linsky, J. L., Margon, B., and Bowyer, S. 1978, *Astr. Ap.*, **70**, 431.
Ayres, T. R., Linsky, J. L., Rodgers, A. W., and Kurucz, R. L. 1976, *Ap. J.*, **210**, 199.
Ayres, T. R., Linsky, J. L., and Shine, R. A. 1975, *Ap. J. (Letters)*, **195**, L121.
Babcock, H. W. 1961, *Ap. J.*, **133**, 572.
Basri, G. S., and Linsky, J. L. 1979, preprint.
Boesgaard, A. M., and Hagen, W. 1974, *Ap. J.*, **189**, 85.
Boggess, A., *et al.* 1978*a*, *Nature*, **275**, 372.
———. 1978*b*, *Nature*,, **275**, 377.
Bohlin, R. C., Holm, A. V., Savage, B. D., Snijders, M. A. J., and Sparks, W. M. 1979, preprint.
Burton, W. M., and Ridgeley, A. 1970, *Solar Phys.*, **14**, 3.
Cohen, L., Feldman, U., and Doschek, G. A. 1978, *Ap. J. Suppl.*, **37**, 393.
Cox, D. P., and Tucker, W. H. 1969, *Ap. J.*, **157**, 1157.
Doherty, L. 1972, *Ap. J.*, **178**, 495.
Doschek, G. A., Feldman, U., Mariska, J. T., and Linsky, J. L. 1978, *Ap. J. (Letters)*, **226**, L35.
Dupree, A. K. 1974, *Bull. A.A.S.*, **6**, 446.
———. 1976, in *Physique des mouvements dans les atmospheres stellaires*, ed. Cayrel and Steinberg (Paris: CNRS), p. 439.
Dupree, A. K., Baliunas, S. L., and Shipman, H. 1977, *Ap. J.*, **218**, 361.
Dupree, A. K., and Shipman, H. L. 1976, *Bull. A.A.S.*, **8**, 394.
Feldman, U., and Doschek, G. A. 1978*a*, *Ap. J. Suppl.*, **37**, 443.
———. 1978*b*, *Astr. Ap.*, **65**, 215.
Feldman, U., Doschek, G. A., Van Hoosier, M. E., and Purcell, J. D. 1976, *Ap. J. Suppl.*, **31**, 445.
Flannery, B. P., and Ayres, T. R. 1978, *Ap. J.*, **221**, 175.
Foukal, P. V. 1975, *Solar Phys.*, **43**, 327.
Gabriel, A. H. 1976, *Phil. Trans. Roy. Soc. London, A*, **281**, 339.
Heath, D. F., and Thekaekara, M. P. 1977, in *The Solar Output and its Variation*, ed. O. R. White (Boulder: Colorado Assoc. Univ. Press), p. 193.
Kamper, K. W., and Wesselink, A. J. 1978, *A.J.*, **83**, 1653.
Kjeldseth Moe, O., and Nicolas, K. R. 1977, *Ap. J.*, **211**, 579.
Kohl, J. L., and Parkinson, W. H. 1976, *Ap. J.*, **205**, 599.
Linsky, J. L., and Ayres, T. R. 1978, *Ap. J.*, **220**, 619.
Linsky, J. L., and Haisch, B. M. 1979, *Ap. J. (Letters)*, **229**, L27.
Linsky, J. L., *et al.* 1978, *Nature*, **275**, 389.
Noyes, R. W. 1971, *Ann. Rev. Astr. Ap.*, **9**, 209.
Nugent, J., and Garmire, G. 1978, *Ap. J. (Letters)*, **226**, L83.
Parker, E. N. 1955, *Ap. J.*, **122**, 293.
Pneuman, G. W. 1973, *Solar Phys.*, **28**, 247.

Pneuman, G. W., and Kopp, R. A. 1978, *Solar Phys.*, **57**, 49.
Pottasch, S. R. 1964, *Space Sci. Rev.*, 3, 816.
Rottman, G. 1978, private communication.
Topka, K., Fabricant, D., Harnden, F. R., Jr., Gorenstein, P., and Rosner, R. 1979, *Ap. J.*, **229**, 661.
Ulmschneider, P. 1970, *Astr. Ap.*, **4**, 144.
Vaiana, G. S., and Rosner, R. 1978, *Ann. Rev. Astr. Ap.*, **16**, 393.
Vernazza, J. E., and Reeves, E. M. 1978, *Ap. J. Suppl.*, **37**, 485.
Vidal-Madjar, A. 1977, in *The Solar Output and Its Variation*, ed. O. R. White (Boulder: Colorado Assoc. Univ. Press), p. 213.
Wilson, O. C. 1978, *Ap. J.*, **226**, 379.
Withbroe, G. L. 1977, in *Proc. OSO 8 Workshop* (Boulder: University of Colorado), p. 2.

THOMAS R. AYRES and JEFFREY L. LINSKY: Joint Institute for Laboratory Astrophysics, University of Colorado, Boulder, CO 80309